

# Aerodynamics Numerical Laboratory

## 2D Project: Hess-Smith

Department of Aerospace Science and Technology (DAER)

Professor: Luca Cortelezzi, Federico Ghioldi

**Matricola Last Name First Name**

225720 Schifone Marco



**POLITECNICO DI MILANO**

Academic Year 2022-2023

December 15, 2022

# Contents

<b>1</b>	<b>Introduction</b>	<b>1</b>
<b>2</b>	<b>Numerical Analysis</b>	<b>1</b>
2.1	Single airfoil problem . . . . .	1
2.2	Tandem configuration . . . . .	3
2.3	Tandem configuration with the ground effect . . . . .	3
2.4	Analysis of the rear wing of an F1 car . . . . .	4

## List of Figures

1	Pressure coefficient for Hess-Smith method and from Xfoil for NACA 2312. . . . .	1
2	Pressure coefficient for Hess-Smith method and from Xfoil for NACA 0012. . . . .	1
3	Lift coefficient for Hess-Smith method and from Xfoil for NACA 2312. . . . .	2
4	Lift coefficient for Hess-Smith method and from Xfoil for NACA 0012. . . . .	2
5	Percentage error in the computation of lift coefficient for NACA 2312. . . . .	2
6	Percentage error in the computation of lift coefficient for NACA 0012. . . . .	2
7	Pressure coefficient for the tandem configuration with $\alpha_w = 2^\circ$ , $\alpha_t = 0^\circ$ . . . . .	3
8	Lift coefficient for wing and tail as $\alpha_t$ changes. . . . .	3
9	Pressure coefficient for the tandem configuration and ground effect with $\alpha_w = 2^\circ$ , $\alpha_t = 0^\circ$ . . . . .	4
10	Lift coefficient for wing and tail as $\alpha_t$ changes. . . . .	4
11	Lift coefficient for wing and tail as the altitude changes. . . . .	4
12	Lift coefficient for the wing as $\alpha_t$ changes. . . . .	4
13	DRS system closed, configuration 1. . . . .	5
14	DRS system open, configuration 1. . . . .	5

## List of Tables

1	Data of the problem. . . . .	1
2	Lift coefficient for the rear wing, configuration 1 . . . . .	5
3	Lift coefficient for the rear wing, configuration 2 . . . . .	5

# 1 Introduction

The main objective of the 2D project is to implement the method of Hess-Smith, in order to study the flow over two airfoils in tandem configuration with the ground effect. The Hess-Smith method is one of the easiest way to formulate a panel method, it is based on a distribution of vortices, whose strength is constant on different panels, and sources, whose strength varies from one panel to another. Moreover the geometry of the airfoil is discretized into different segments, called panels, on which is defined a control point, placed in the middle of each panel.

For each airfoil, if  $N$  is the number of panels, we will have  $N + 1$  unknowns, which will be found by imposing  $N$  boundary condition and the Kutta condition at the trailing edge. When using the Hess-Smith method we need to remember the hypothesis made: the flow is considered as incompressible, inviscid and irrotational. Then, the results will be accurate if only the camber and the thickness of the profile is small as well as the angle of attack, in order to avoid problems connected to the separation of the flow, which can't be studied by means of this method.

Furthermore, we are also ignoring the effects of the thickness distribution of  $c_L$ .

The code for the problem of the single airfoil can be modified in order to study other relevant problems, among which we can find the tandem configuration and the influence of the ground effect.

Firstly will be provided the study of the two single airfoils, then we will study the tandem configuration with and without the ground effect and then will be changed the angle of attack of the tail  $\alpha_t$  in order to maximize the  $c_L$  of the front wing.

It won't be investigated the problem of computational space necessary to run the code, because it is not relevant in this simple code. The data of the problem are shown in table 1.

$$\begin{array}{lll} \alpha_w & = & 2 \\ y_{1,2} & = & 0.12 \text{ m} \end{array} \quad \begin{array}{lll} x_{1,2} & = & 1.25 \text{ m} \\ h & = & 0.23 \text{ m} \end{array}$$

Table 1: Data of the problem.

# 2 Numerical Analysis

## 2.1 Single airfoil problem

In order to validate the code we compare the results obtained with the NACA 2312, which is the main wing, and the NACA 0012, which is the tail, with the results coming from the program Xfoil for the plot of the pressure and lift coefficient  $c_p$ ,  $c_L$ , because it allows us to show the results for the inviscid problem.

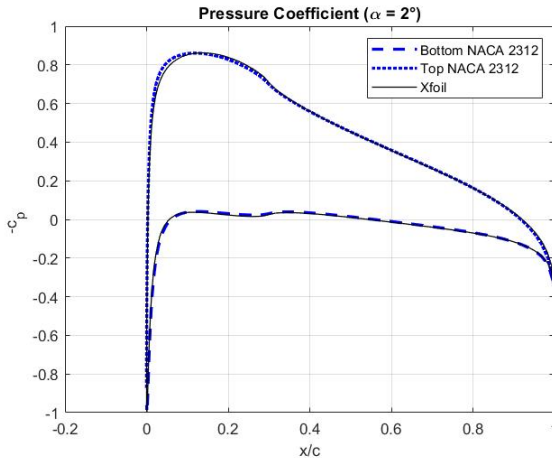


Figure 1: Pressure coefficient for Hess-Smith method and from Xfoil for NACA 2312.

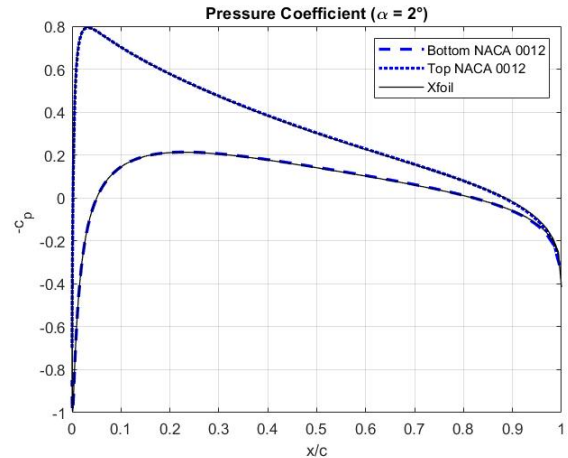


Figure 2: Pressure coefficient for Hess-Smith method and from Xfoil for NACA 0012.

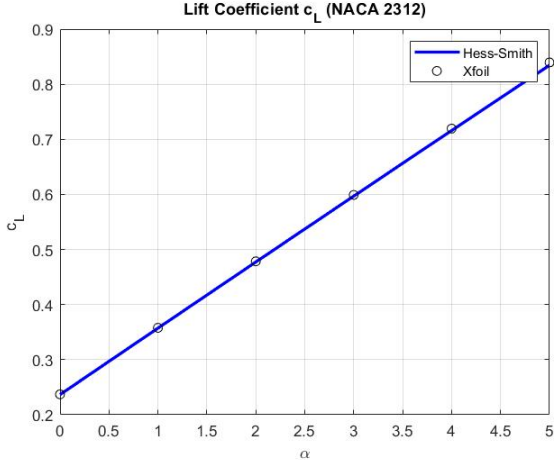


Figure 3: Lift coefficient for Hess-Smith method and from Xfoil for NACA 2312.

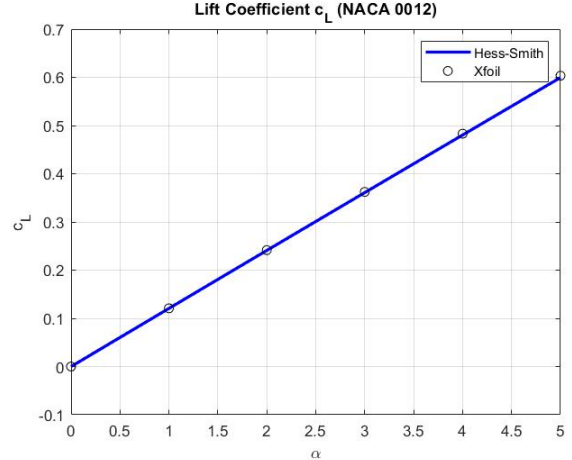


Figure 4: Lift coefficient for Hess-Smith method and from Xfoil for NACA 0012.

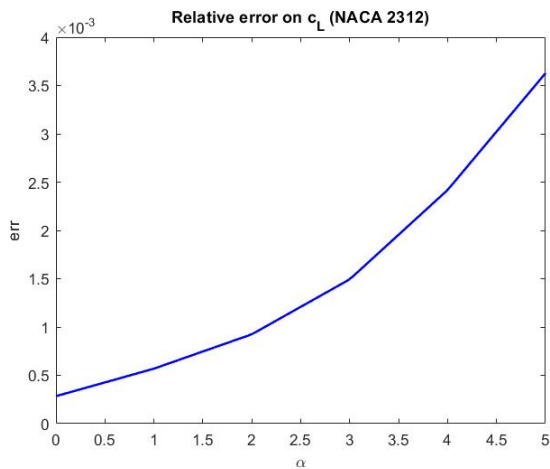


Figure 5: Percentage error in the computation of lift coefficient for NACA 2312.

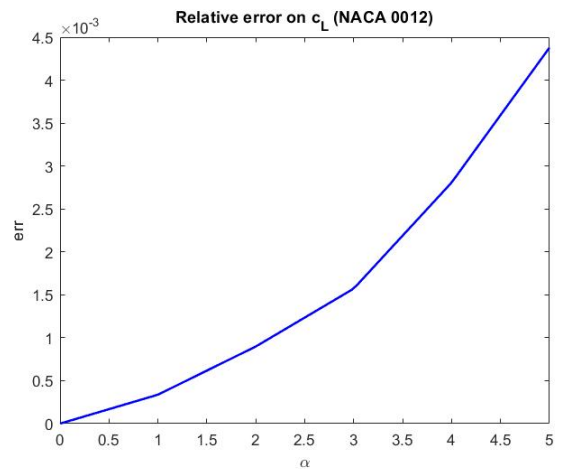


Figure 6: Percentage error in the computation of lift coefficient for NACA 0012.

In Figure 1, 2 it is shown the evolution of the pressure coefficient of the two profiles along the chord at the angle of attack of  $\alpha = 2^\circ$ , it is also represented the  $c_p$  obtained with the program Xfoil, whose evolution is very close to the one found with our analysis. Similarly, in Figure 3, 4 the evolution of the lift coefficient along the chord is shown. The lift coefficient of the wing and tail at the angle of attack of  $\alpha = 2^\circ$  is  $c_{L,w} = 0.4772$ ,  $c_{L,t} = 0.2408$ .

From the results obtained it is clear that the Hess-Smith method can approximate well the performance of the airfoils in this configuration, and by computing the percentage error of the lift coefficient it appears that it is always smaller than the 1%, so we can conclude that our approximation is satisfactory as for this configuration.

Moreover, it is important to highlight that the evolution of the lift coefficient by means of the Hess-Smith method is linear with the angle of attack, due to the inviscid flow approximation, so the range of  $\alpha$  in which our approximation is valid is small, because we can't predict the effects of separation and stall. If we analyze the flow over the airfoil with the program XFLR5, which allows to perform a simulation of the problem with the influence of the viscosity, it is possible to notice that the stall angle of the tail is close to the value of  $\alpha_t = 10^\circ$ , so in our analysis we will consider the maximum angle of attack of the tail as  $\alpha_t = 9^\circ$ .

## 2.2 Tandem configuration

Now we are considering the tandem configuration with a prescribed distance from the main wing to the tail, where we define  $x_{1,2}$  as the distance from the leading edge of the wing to the leading edge of the tail, whereas  $y_{1,2}$  it is the vertical distance from the two airfoils, which is taken from the trailing edge of the wing to the leading edge of the tail.

Then we can compute the  $c_p$  and  $c_L$  for the tandem configuration with the first profile at the same angle of attack  $\alpha_w = 2^\circ$ , whereas the one of the tail is null.

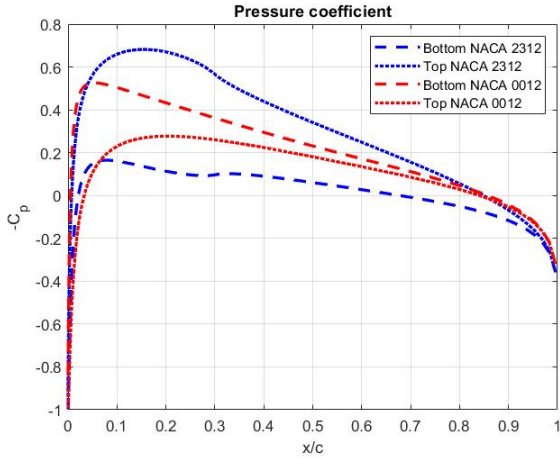


Figure 7: Pressure coefficient for the tandem configuration with  $\alpha_w = 2^\circ$ ,  $\alpha_t = 0^\circ$ .

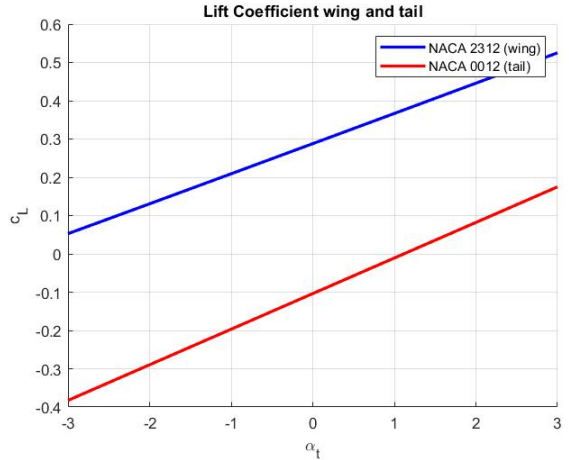


Figure 8: Lift coefficient for wing and tail as  $\alpha_t$  changes.

As it could have been expected the lift coefficient of the wing increases as the angle of attack of the tail increases. This means that it is possible to increase  $c_{L,w}$  at a fixed angle of attack of the wing, thanks to the introduction of the tail and by changing its the angle of attack. The resultant lift coefficients for the wing and the tail, at the angle of attack of  $\alpha_w = 2^\circ$ ,  $\alpha_t = 0^\circ$ , are:  $c_{L,w} = 0.2879$ ,  $c_{L,t} = -0.1037$ .

## 2.3 Tandem configuration with the ground effect

Now we are introducing the ground effect on the tandem configuration, with which we will expect to measure an increase in the lift of the main wing. So we are using the same configuration and angle of attack for the wing, whereas the angle of attack of the tail varies in the range from  $\alpha_t = -2^\circ$  to  $\alpha_t = 4^\circ$ .

From the results shown in Figure 9, 10 it is possible to notice an increase in the value of the lift produced by both the main wing and the tail. The lift coefficients, obtained for the following values of angle of attack  $\alpha_w = 2^\circ$ ,  $\alpha_t = 0^\circ$ , are  $c_{L,w} = 0.8897$ ,  $c_{L,t} = 0.1253$ .

Now it can be interesting to evaluate how the lift coefficient changes with the distance from the ground, with the same configuration considered before of  $\alpha_w = 2^\circ$ ,  $\alpha_t = 0^\circ$ , the results are shown in Figure 11. Once all of these cases are analyzed, now it is possible to find the value of the angle of attack of the tail, which maximizes the lift coefficient of the wing. In Figure 12 are presented the results of this analysis, thanks to which it is possible to find that the value of  $\alpha_t = 9^\circ$  corresponds to the maximum value of the lift coefficient of the wing, which is  $c_{L,max} = 1.1511$ .

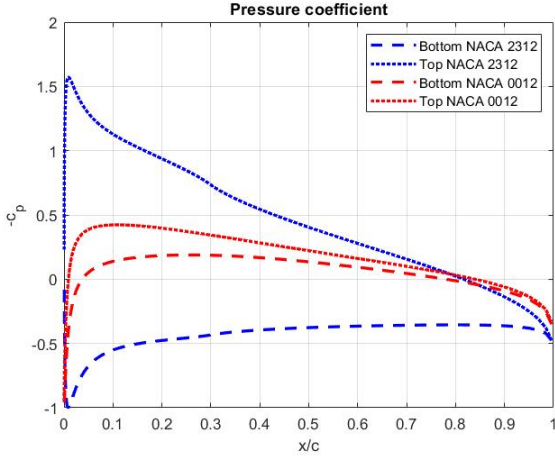


Figure 9: Pressure coefficient for the tandem configuration and ground effect with  $\alpha_w = 2^\circ$ ,  $\alpha_t = 0^\circ$ .

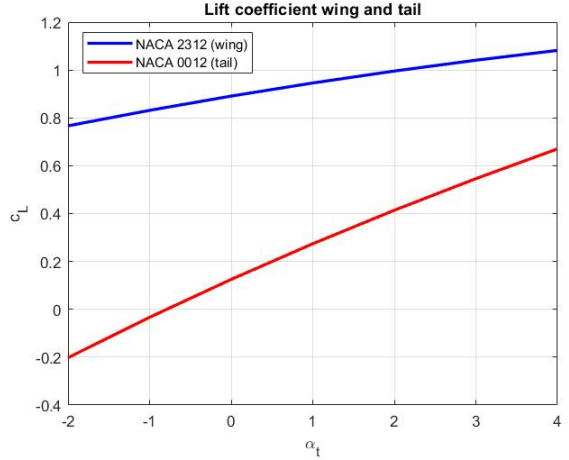


Figure 10: Lift coefficient for wing and tail as  $\alpha_t$  changes.

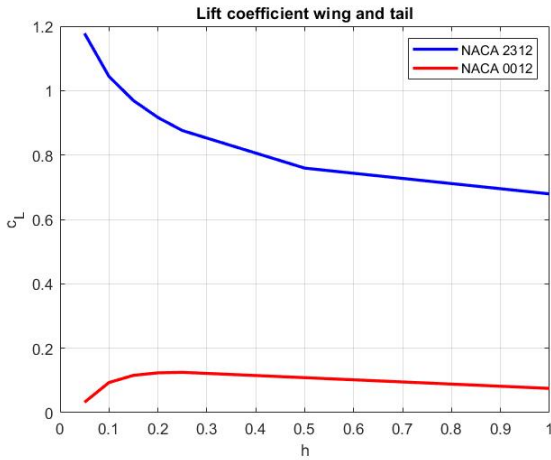


Figure 11: Lift coefficient for wing and tail as the altitude changes.

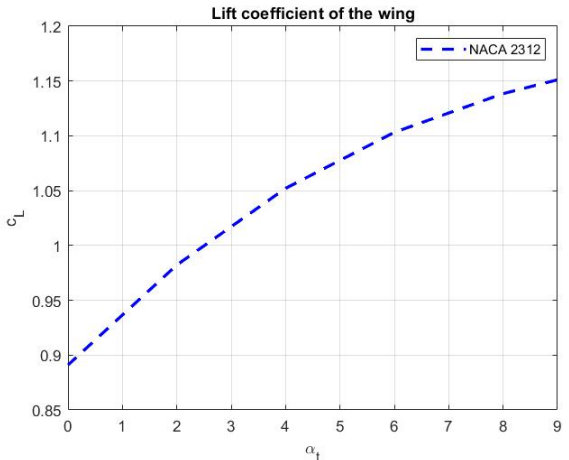


Figure 12: Lift coefficient for the wing as  $\alpha_t$  changes.

## 2.4 Analysis of the rear wing of an F1 car

Now we can apply our code to a slight different case: since we are now dealing with cars, the main objective is to produce downforce instead of lift, so we need to consider different airfoils. In order to simplify the analysis, we will consider also in this case NACA profiles, in particular the NACA 6407 will be chosen for both the main wing and the flap, but they will be considered upside down, in order to create downforce with a null angle of attack. Moreover, it is important to highlight the fact that the rear wing of an F1 produces more or less the 20% of the total downforce of the car, but it also produces a huge quantity of drag. To increase the maximum speed on the straights the DRS (Drag Reduction System) was introduced. The DRS system allows to open an adjustable flap on the rear wing, in order to reduce the drag produced by the wing, but reducing the downforce as well. Due to the hypothesis of inviscid flow, this reduction of drag can't be evaluated by means of this method, so it will be only analyzed the reduction in the overall downforce of the rear wing.

The angle of attack of the main wing is  $\alpha_w = -4^\circ$ , the one of the flap is  $\alpha_f = -28^\circ$  when the flap is in the closed position. Moreover, due to restrictions of the technical regulations, we must have at least a vertical distance of  $y_{closed} = 10$  mm when the flap is closed, and a maximum distance of  $y_{open} = 50$  mm when it is open. The hinge is now moved to the 80% of the chord, in order to facilitate the deployment of the DRS system. For our first analysis we will choose the two airfoils with the same chord.

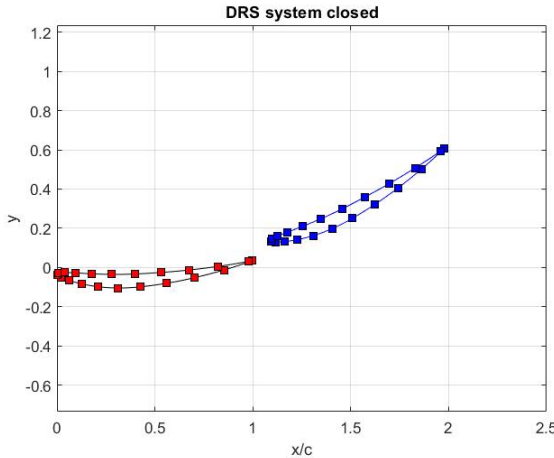


Figure 13: DRS system closed, configuration 1.

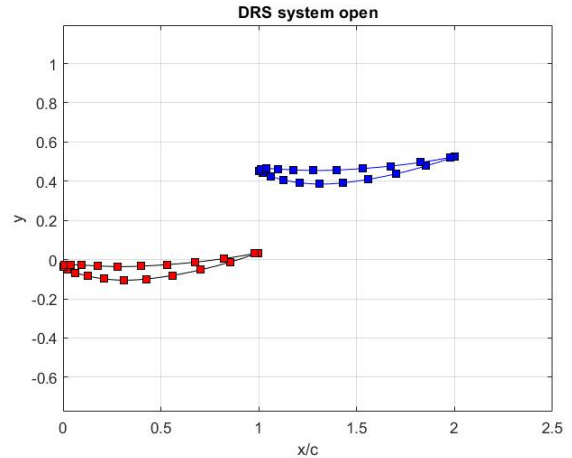


Figure 14: DRS system open, configuration 1.

Flap position	$c_{L,wing}$	$c_{L,flap}$
Open	-1.6362	-0.5570
Closed	-3.8389	-2.1317

Table 2: Lift coefficient for the rear wing, configuration 1

The results of this analysis are shown in Table 2, and as we would have expected the reduction of the lift coefficient of the wing is substantial when the flap is open, with a decreasing in the  $c_{L,w}$  of the 57.38%, whereas the reduction of the lift coefficient of the flap is more consistent and its value is 73.87%.

Now we are considering a different configuration, by changing the length of the chord of the flap. The chord of the wing is now  $c_{wing} = 0.320$  mm, meanwhile the length of the chord of the flap is  $c_{tail} = 0.192$  mm. The angle of attack of the main wing is fixed at  $\alpha_w = -4^\circ$ , whereas the angle of attack of the flap is  $\alpha_f = -4^\circ$  when the DRS is open, and  $\alpha_f = -28^\circ$  when the DRS is closed. Since changing considerably the camber of the airfoil it is not possible in the Hess-Smith analysis, the configuration 2 of the rear wing can be seen as a low-downforce configuration, due to the lowered chord of the flap.

The results of the analysis are shown in Table 3, from which it is possible to notice a global reduction of the lift coefficient with respect to configuration 1. Moreover, if we compute the percentage decrease of the lift coefficient from the closed to the open configuration, we can find that the lift coefficient of the wing is subjected to a 52.02% reduction, the one of the flap to a reduction of the 77.83%.

Flap position	$c_{L,wing}$	$c_{L,flap}$
Open	-1.4861	-0.2695
Closed	-3.0971	-1.2159

Table 3: Lift coefficient for the rear wing, configuration 2